# 11.7 QUALITY CONTROL OF RADIOSONDE MOISTURE OBSERVATIONS

Seth I. Gutman[*1], Joseph Facundo[*2], David Helms[*3]

[1]GPS-Met Observing Systems Branch, NOAA/OAR Forecast Systems Laboratory, Boulder, CO
[2] Observing Systems Branch, NOAA/NWS Office of Operational Systems, Silver Spring, MD
[3] Science Plans Branch, NOAA/NWS Office of Science and Technology, Silver Spring, MD

## 1. INTRODUCTION

Integrated (total atmospheric column) precipitable water vapor (IPW) is now routinely retrieved in near real-time from data acquired at more then 300 Global Positioning System (GPS) sites in North America. The coverage (Figure 1) allows routine comparisons of IPW calculated using GPS signal delay estimates (1)

$$\mathrm{IPW} = \frac{1}{\Pi}\left[\mathrm{ZTD} - \mathrm{ZHD}\right] \qquad (1)$$

where:
ZTD = zenith tropospheric delay (Duan et al., 1996)
ZHD = zenith hydrostatic delay (Bevis et al., 1992)
$\Pi$ = wet delay transfer function (Bevis et al., 1994).

to be made with the same quantity calculated using radiosonde moisture soundings (2).

$$\mathrm{IPW} = \frac{1}{g}\int_{P_{sfc}}^{0} \omega_v \, dP \qquad (2)$$

where:
g = gravitational acceleration
$\omega_v$ = water vapor mixing ratio
P = atmospheric pressure

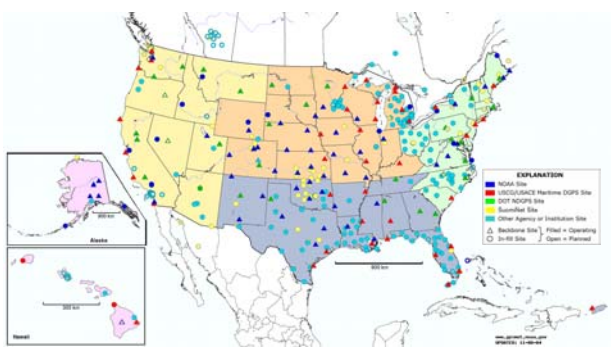

**Fig 1. NOAA GPS-Met network currently consists of 318 sites, 22 of which are within 10 km of an Upper-Air sites. 17 of these sites were used in a one-year evaluation of GPS and radiosonde IPW observations described in this paper.**

The result is that a 21st century upper-air observing system (GPS) can be used with a 60 year-old technology (radiosondes) to improve numerical weather prediction, global climate monitoring, and satellite remote sensing.

* Corresponding author address: Seth I. Gutman, NOAA Forecast Systems Laboratory, 325 Broadway R/FS3, Boulder, CO 80305-3328; e-mail: Seth.I.Gutman@noaa.gov; web: http://gpsmet.noaa.gov.

### 1.1 GPS Meteorology

The techniques to use GPS to measure IPW in the troposphere were first articulated by Bevis et al. (1992, 1994) and Duan et al. (1996). Since 1994, the NOAA Forecast Systems Laboratory in Boulder, CO has been making continuous GPS measurements at a growing number of sites to demonstrate the major aspects of an operational GPS integrated precipitable water vapor (IPW) monitoring system. Other goals associated with the NOAA Research project are to assess the impact of GPS data on weather forecasts, assist in the transition of these techniques to operational use within NOAA, and encourage the use of GPS meteorology for atmospheric research and other applications. The implementation of ground-based GPS-Meteorology within NOAA has been described in several papers, including by Wolfe and Gutman (2000), and Gutman et al. (2004a). The accuracy with which these observations can be realistically made under operational conditions was discussed by Gutman et al., 2004b.

The first and most mature use of GPS for atmospheric remote sensing is for the measurement of IPW directly above GPS continuously operating reference station (CORS) sites. A network of nearly 500 CORS sites across the U.S. was established by NOAA's National Geodetic Survey (http://ngs.noaa.gov/CORS) to improve the National Spatial Reference System and facilitate high accuracy positioning and navigation throughout America. Due to a fortuitous synergy between the GPS receiver requirements for high accuracy positioning and atmospheric remote sensing, the CORS network forms the backbone of the NOAA GPS-Met network.

At approximately the same time that the use of total precipitable water vapor measurements from ground-based GPS receivers for atmospheric remote sensing was proposed by Bevis et al. 1992, Kursinski et al. (1993) described the use of GPS radio occultation (RO) techniques for temperature and moisture sounding, and Yuan et al. (1993) discussed the utility of RO measurements for climate change detection and monitoring.

From a geometric standpoint, RO measurements (Figure 2) are like ground-based measurements turned on their side (Figure 3). The fundamental measurement in both cases is:

$$L_S = \int n_S ds \qquad (3)$$

where:

$L_S$ = the excess path length caused by the total refractivity of the atmosphere, and

$n_S$ = refractive index along the path s

and the total refractivity is assumed to have only three components:

- An ionospheric component caused by the total electron content (TEC) of the upper atmosphere;
- A dry component caused by the mass of the atmosphere;
- A wet component caused by water vapor in the lower atmosphere.

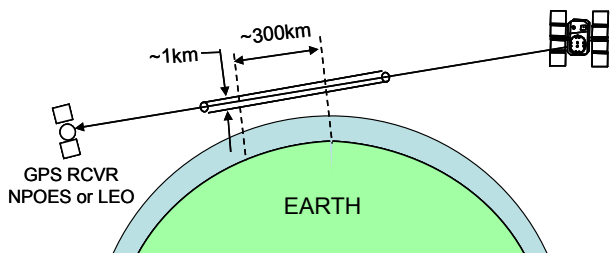


**Fig 2. Radio occultation geometry. The GPS radio signal is bent and slowed as it passes through the atmosphere. In the upper atmosphere, slowing and bending is a function of the total electron content (TEC) of the ionosphere. This parameter is used in Space Weather forecasting because TEC is a tracer for geomagnetic storm activity. In the lower atmosphere, slowing and bending is a function of temperature, pressure, and water vapor which increases as the GPS receiver in a Low Earth Orbiting satellite rises or sets behind the limb of the Earth.**

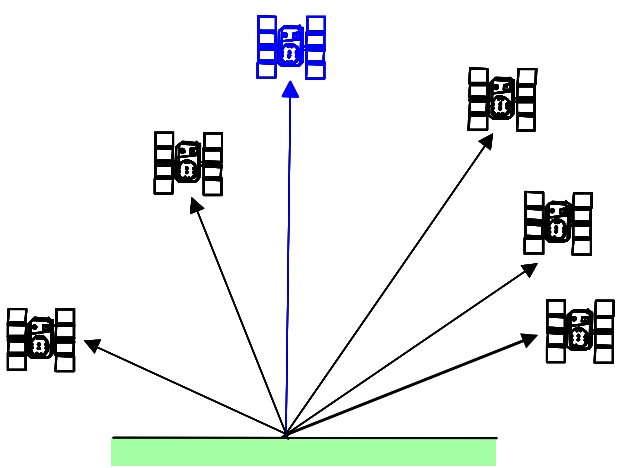

**Fig 3. Ground-based GPS-Met geometry. The delays from all GPS satellites in view (black) are scaled to the zenith (blue) and averaged to reduce line of sight (slant-path) tropospheric delay error. With 6-10 satellites in view at all times, the solution for the zenith tropospheric signal delay is over-determined, and can be estimated with high accuracy. Ground-based GPS Met retrievals represent a volumetric average within a region of about 11 km of the antenna. As such, ground-based GPS-Met observations have much in common with satellite brightness temperature measurements.**

### 1.2 Application to Integrated Observing Systems

All GPS-Met techniques, regardless of measurement strategy, provide only path integrated measurements of total refractivity. In RO, the technique provides more-or-less vertical refractivity profiles while in ground-based techniques, a single estimate of the total zenith refractivity is derived. Retrieval of physical parameters from these measurements (e.g. temperature or water vapor) require additional information or constraint, since there is no unique solution to the Smith-Weintraub equation (Smith and Weintraub, 1953).

In ground-based GPS Meteorology, this external constraint usually comes from the measurement of surface pressure which maps directly into the zenith-scaled hydrostatic signal delay in (1) (Saastamoinen, 1972). Alternatively, ZTD or RO measurements can be directly assimilated into atmospheric models using the general variational technique described by Eyre (1994).

As originally conceived by the NOAA Forecast Systems Laboratory, GPS IPW measurements would primarily be used as a proxy for moisture soundings in numerical weather prediction models. Ground-based GPS Meteorology (GPS-Met) sensors were designed to provide data at high (ultimately arbitrary) temporal resolution for the most demanding data assimilation requirement: a rapid refresh model such as the operational Rapid Update Cycle or the planned rapid-refresh version of the Weather Research and Forecasting (WRF) model.

As such, GPS observations were and are still seen as complementing the primary sources of atmospheric moisture: radiosondes, surface measurements, and satellite observations.

The majority of the information about the vertical distribution of water vapor in the atmosphere comes from radiosondes that make in-situ measurements twice daily at widely spaced locations. This permits resolution of regional-scale features fairly well, but is inadequate to resolve many small-scale variations associated with severe weather. A large number of surface measurements of dew point temperature (convertible to relative humidity) are made hourly at land sites throughout the world, mostly at airports, but these tell us very little about what is happening with respect to moisture in the atmosphere above the surface. Finally, information from satellite observations is also available, but these data also have limitations. In general, satellite-based water vapor estimates derived from upwelling infrared radiation have high horizontal resolution but course vertical resolution, and are reliable only in cloud-free regions. Multispectral satellite measurements made at various frequencies emitted by water vapor also provide additional information about water vapor above approximately 5 km above the

earth's surface (below ~550 hPa isobaric level), but again with coarse vertical resolution. Water vapor estimates derived from space-born microwave radiometers in polar orbit are available every six hours and are valid in cloudy regions, but are generally reliable only over open water.

Estimates of IPW derived from GPS signal delays complement these other atmospheric moisture observation sources in several ways. In general, there is almost no redundancy today in upper-air moisture observations. Even when routine moisture observations are made by commercial aircraft carrying sensors such as the Water Vapor Sensing System (WVSS-II) (http://www.joss.ucar.edu/wvss/spectrasensors.pdf) and the Tropospheric Airborne Meteorological Data Reporting (TAMDAR) system (http://www.airdat.com/), observation verification and quality control of radiosondes, satellites and aircraft observations will continue to be essential. GPS-Met, working synergistically with these and other observing systems can provide ongoing independent verification of moisture observations for the foreseeable future. In fact, one attribute of GPS that makes it almost ideal for this application is that it requires no external calibration. The reason for this is that the signal delays are estimated by measuring the time of flight of the GPS radio signals as they travel from space to the receivers on the ground. This measurement is fundamentally tied to the accuracy of the atomic clocks in the satellites which continue to improve (not degrade) with time. In principle, this provides us with a temporally invariant reference for global climate observations.

One of the most valuable attributes of GPS IPW is its ability to provide accurate signal delay estimates under all weather conditions. From a forecasting perspective, GPS PWV observations are most valuable when satellites cannot obtain good radiance measurements, mainly in cloudy regions where the need for accurate measurements is greatest since areas of precipitation are also cloudy. The reason this is possible is because GPS and other Global Navigation Satellite Systems (GNSS) such as the planned European Union Galileo GNSS will broadcast radio signals in the L-band portion of the electromagnetic spectrum that is essentially transparent to liquid water.

The ability to do this was clearly demonstrated in September, 2004 when Hurricanes Francis made landfall along the Gulf Coast of Florida (Figure 4). This event was monitored by a GPS-Met system in Tallahassee, FL that measured 7.57 cm (2.98 inches) of precipitable water vapor in the atmosphere: a record that stood for about one week when Hurricane Ivan came ashore near Mobile, and 80.4 mm (3.16") was measured at Mobile Point.

Finally, other objective and subjective uses of GPS have emerged that deserve passing mention. These applications generally involve the need for independent measurements to verify other observations, verify (NWP and climate) model analyses and predictions, and to calibrate, validate and/or quality control observations, especially from nadir-looking remote sensing platforms such as satellites and aircraft. The latter topic is

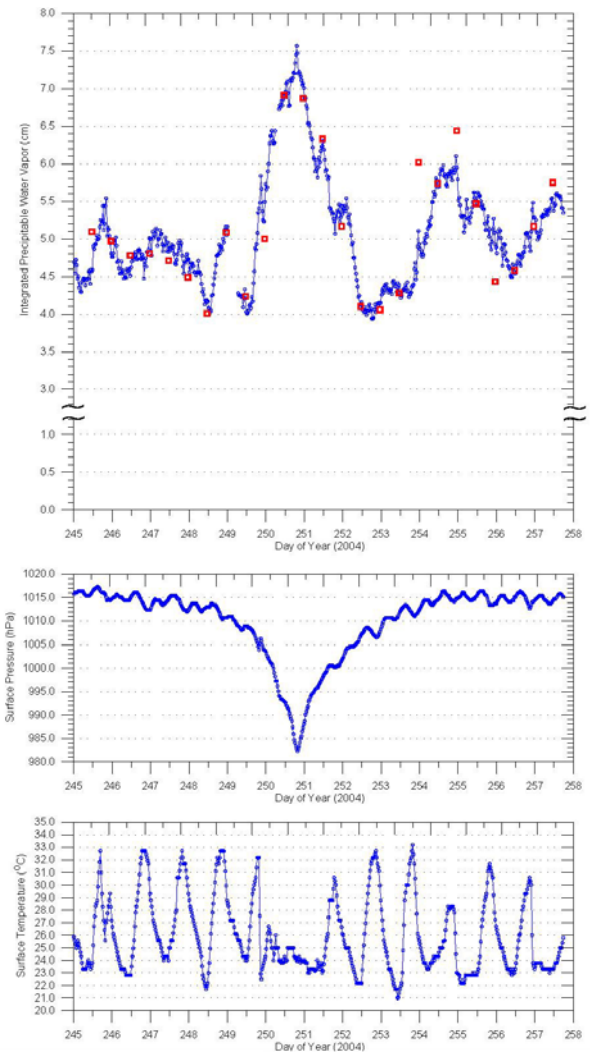


**Fig 4. Integrated precipitable water vapor, surface pressure and temperature measured at Tallahassee, FL during the passage of Hurricane Francis in 2004. The red squares in the upper panel are precipitable water vapor measured by radiosondes launched at the NWS Upper Air facility TLH.**

covered in detail in (McMillin et al., 2005), paper 1.3 in the 9th Symposium on Integrated Observing and Assimilation Systems for the Atmosphere, Oceans, and Land Surface (IOAS-AOLS).

## 2. COMPARISON OF OPERATIONAL RADIOSONDES AND GPS WATER VAPOR MEASUREMENTS

After more than 60 years, measurements made by radiosondes still provide the standard upper-atmospheric data set for numerical weather prediction, regional weather forecasting, climatology, research, and other applications. Radiosonde measurements also form the basis of inter-comparison, calibration and validation of most other atmospheric observing systems,

and serve as the benchmark or "ground-truth" for satellite-derived estimates of temperature, moisture and other atmospheric parameters. Because of the unique characteristics of radiosonde observations and the fact that many of the parameters measured by radiosondes (e.g. moisture) are poorly observed by other techniques, verification of radiosonde soundings can be difficult under some circumstances (Gutman et al., 2004b).

To assess the relative behavior of GPS and operational radiosondes, and determine if GPS-IPW measurements could be used to reliably detect questionable radiosonde moisture soundings, we identified 17 GPS sites within 10 km of an upper-air facility (Table 1 and Figure 5) and calculated IPW differences (sonde-GPS) for one year between August 1, 2003 and July 31, 2004.

**Table 1. GPS-Met sites within 10 km of an Upper-Air site**

| SITE | ST | GPS | RAOB | LAT | LON | HORZ (km) | VERT (m) |
|---|---|---|---|---|---|---|---|
| 1 - Jacksonville | FL | jxvl | jax | 30.80 | -81.70 | 0.50 | 1.9 |
| 2 - Tallahassee | FL | talh | tlh | 30.40 | -84.36 | 0.60 | 2.3 |
| 3 - Key West | FL | kwst | eyw | 24.55 | -81.75 | 0.60 | 3.9 |
| 4 - Blacksburg | VA | blkv | rnk | 37.21 | -80.41 | 0.80 | 5.4 |
| 5 - Hilo | HI | hilo | hto | 19.72 | -155.05 | 0.80 | 0.1 |
| 6 - Flagstaff | AZ | fst1 | fgz | 35.22 | -11.82 | 0.90 | 22.1 |
| 7 - Salt Lake City | UT | slcu | slc | 40.77 | -111.19 | 1.00 | 5.6 |
| 8 - Cape Canaveral | FL | ccv3 | xrb | 28.46 | -80.55 | 1.20 | 6.2 |
| 9 - Pago Pago | AS | aspa | stu | -14.33 | -170.27 | 1.60 | 48.2 |
| 10 - Anchorage | AK | anc1 | anc | 61.18 | -150.00 | 2.90 | 3.2 |
| 11 - Grand Junction | CO | mc01 | gjt | 39.09 | -108.53 | 3.20 | 17.8 |
| 12 - Lake Charles | LA | mcne | lch | 30.18 | -93.22 | 5.60 | 12.1 |
| 13 - Bismarck | ND | bsmk | bis | 46.82 | -100.82 | 7.10 | 67.5 |
| 14 - Point Barrow | AK | sg27 | brw | 71.32 | -156.61 | 7.70 | 0.1 |
| 15 - Corpus Christi | TX | txcc | crp | 27.74 | -97.44 | 8.00 | 1 |
| 16 - Vandenberg AFB | CA | van1 | vbg | 34.83 | -120.56 | 8.50 | 13.7 |
| 17 - Gaylord | MI | nor2 | apx | 44.99 | -84.68 | 9.30 | 53.5 |

**Fig 5. 17 Upper-Air sites within 10 km of a GPS water vapor system that were evaluated for one year as part of this study. Two other sites (18 and 19) were evaluated separately as part of a continuing evaluation of the Radiosonde Replacement System (RRS) performed in collaboration with the Observing Systems Branch of the NWS Office of Operational Systems (See Fitzgibbon and Facundo, 2005.)**

Selecting the best time to compare GPS and radiosonde observations can be extremely important, especially during active weather conditions. Rather then use the nominal launch time of 0 UTC and 12 UTC, we elect to use the actual launch times of 2315 UTC and 1115 UTC for our comparisons. Our reasoning is that since the average balloon rise rate is about 300 m/min, the radiosonde has sampled more then 90% of the moisture in the troposphere by the time it reaches 4,500 m (about 600 hPa) 15 minutes after launch. In general, this is more representative of the moisture sampled by the GPS in the observation session between 1100 and 1130 UTC (for example) then it is 45 minutes later.

Table 2 contains the summary statistics for all radiosonde and GPS observation comparisons made between August 1, 2003 and July 31, 2004 at the 17 sites identified in Table 1. The variables are defined as follows: Num = the number of matched pairs; Min = the minimum difference (raob-GPS) in cm; Max = the maximum difference in cm; Mean = the arithmetic mean of the differences in cm; Sigma = the standard deviation of the differences in cm; RMS = the root mean square differences in cm; and Corr = the correlation coefficient between the raob measurements on the ordinate and GPS measurements on the abscissa. Table 3 presents the summary statistics in Table 2 minus "outliers" defined as all measurements greater than ±2 root mean square differences (RMSD) between sonde and GPS measurements.

**Table 2. Summary statistics derived from the differences between all integrated radiosonde moisture soundings and GPS integrated precipitable water vapor measurements made at the 17 upper-air sites identified in Table 1 between August 1, 2003 and July 31, 2004.**

| SITE | ST | GPS | RAOB | Num | Min | Max | Mean | Sigma | RMS | Corr |
|---|---|---|---|---|---|---|---|---|---|---|
| 1 - Jacksonville | FL | jxvl | jax | 669 | -1.89 | 1.95 | -0.0019 | 0.2226 | 0.2224 | 0.9901 |
| 2 - Tallahassee | FL | talh | tlh | 637 | -1.22 | 1.83 | -0.0083 | 0.1984 | 0.1985 | 0.9920 |
| 3 - Key West | FL | kwst | eyw | 661 | -0.99 | 1.16 | 0.1273 | 0.2533 | 0.2833 | 0.9824 |
| 4 - Blacksburg | VA | blkv | rnk | 684 | -1.53 | 2.98 | 0.0597 | 0.2053 | 0.2137 | 0.9858 |
| 5 - Hilo | HI | hilo | hto | 366 | -2.6 | 1.34 | -0.0485 | 0.3446 | 0.3475 | 0.8759 |
| 6 - Flagstaff | AZ | fst1 | fgz | 656 | -2.02 | 0.66 | -0.0249 | 0.1515 | 0.1534 | 0.9683 |
| 7 - Salt Lake City | UT | slcu | slc | 716 | -1.21 | 1.62 | -0.0245 | 0.1726 | 0.1742 | 0.9630 |
| 8 - Cape Canaveral | FL | ccv3 | xrb | 385 | -1.26 | 1.03 | 0.2575 | 0.2898 | 0.3874 | 0.9818 |
| 9 - Pago Pago | AS | aspa | stu | 565 | -2.94 | 2.6 | -0.0102 | 0.4745 | 0.4742 | 0.8909 |
| 10 - Anchorage | AK | anc1 | anc | 681 | -0.883 | 1.007 | -0.0281 | 0.1273 | 0.1303 | 0.9839 |
| 11 - Grand Junction | CO | mc01 | gjt | 572 | -0.5 | 0.71 | -0.0188 | 0.1068 | 0.1083 | 0.9861 |
| 12 - Lake Charles | LA | mcne | lch | 621 | -3.45 | 2.56 | 0.0979 | 0.3483 | 0.3615 | 0.9736 |
| 13 - Bismarck | ND | bsmk | bis | 686 | -1.6 | 0.64 | -0.1337 | 0.1742 | 0.2195 | 0.9792 |
| 14 - Point Barrow | AK | sg27 | brw | 543 | -1.4 | 0.46 | 0.0375 | 0.1179 | 0.1236 | 0.9713 |
| 15 - Corpus Christi | TX | txcc | crp | 653 | -1.17 | 2.85 | 0.0981 | 0.3168 | 0.3314 | 0.9739 |
| 16 - Vandenberg AFB | CA | van1 | vbg | 591 | -1.97 | 1.76 | 0.1169 | 0.3887 | 0.3419 | 0.7711 |
| 17 - Gaylord | MI | nor2 | apx | 675 | -1.22 | 2.12 | -0.0306 | 0.1902 | 0.1925 | 0.9804 |
| Average of all sites | | | | 609 | -1.64 | 1.60 | 0.03 | 0.24 | 0.25 | 0.96 |

**Table 3. Summary statistics from Table 2 minus "outliers" defined as all measurements greater than ±2 root mean square differences (RMSD) between sonde and GPS measurements.**

| SITE | ST | GPS | RAOB | Num | Min | Max | Mean | Sigma | RMS | Corr |
|---|---|---|---|---|---|---|---|---|---|---|
| 1 - Jacksonville | FL | jxvl | jax | 643 | -0.44 | 0.44 | -0.0025 | 0.1390 | 0.1389 | 0.9961 |
| 2 - Tallahassee | FL | talh | tlh | 617 | -0.39 | 0.38 | -0.0184 | 0.1265 | 0.1277 | 0.9967 |
| 3 - Key West | FL | kwst | eyw | 626 | -0.56 | 0.56 | 0.1084 | 0.2073 | 0.2338 | 0.9883 |
| 4 - Blacksburg | VA | blkv | rnk | 665 | -0.42 | 0.4 | 0.0518 | 0.1069 | 0.1187 | 0.9961 |
| 5 - Hilo | HI | hilo | hto | 355 | -0.66 | 0.69 | -0.0360 | 0.2696 | 0.3329 | 0.9288 |
| 6 - Flagstaff | AZ | fst1 | fgz | 634 | -0.3 | 0.28 | -0.0168 | 0.0844 | 0.0860 | 0.9897 |
| 7 - Salt Lake City | UT | slcu | slc | 693 | -0.33 | 0.34 | -0.0329 | 0.1011 | 0.1062 | 0.9869 |
| 8 - Cape Canaveral | FL | ccv3 | xrb | 370 | -0.63 | 0.77 | 0.2441 | 0.2536 | 0.3517 | 0.9860 |
| 9 - Pago Pago | AS | aspa | stu | 541 | -0.94 | 0.93 | -0.0259 | 0.1171 | 0.2249 | 0.9429 |
| 10 - Anchorage | AK | anc1 | anc | 664 | -0.263 | 0.24 | -0.0290 | 0.0984 | 0.1025 | 0.9901 |
| 11 - Grand Junction | CO | mc01 | gjt | 535 | -0.21 | 0.2 | -0.0133 | 0.0723 | 0.0734 | 0.9928 |
| 12 - Lake Charles | LA | mcne | lch | 601 | -0.69 | 0.71 | 0.0914 | 0.1898 | 0.2106 | 0.9920 |
| 13 - Bismarck | ND | bsmk | bis | 661 | -0.43 | 0.41 | -0.1216 | 0.1411 | 0.1861 | 0.9861 |
| 14 - Point Barrow | AK | sg27 | brw | 524 | -0.22 | 0.24 | 0.0352 | 0.0866 | 0.0934 | 0.9852 |
| 15 - Corpus Christi | TX | txcc | crp | 628 | -0.59 | 0.65 | 0.0817 | 0.2498 | 0.2626 | 0.9840 |
| 16 - Vandenberg AFB | CA | van1 | vbg | 543 | -0.68 | 0.68 | 0.0623 | 0.2838 | 0.2903 | 0.8707 |
| 17 - Gaylord | MI | nor2 | apx | 657 | -0.38 | 0.38 | -0.0378 | 0.1015 | 0.1082 | 0.9943 |
| **Average of all sites** | | | | **586** | **-0.48** | **0.49** | **0.02** | **0.15** | **0.18** | **0.98** |

Figure 6 is plotted from the values presented in Tables 2 and 3, with the sites ordered by increasing mean IPW difference (radiosonde minus GPS). With this convention, the radiosondes launched at Bismarck, ND and Cape Canaveral, FL are the driest and wettest with respect to independent GPS observations.

There are no apparent correlations between radiosonde and GPS differences based on horizontal distance. The only correlation based on vertical offset is seen at Bismarck, ND where the dry bias can be explained by the physical setting and relatively large vertical distance between the Upper-Air Site at the airport and the GPS receiver in Missouri River Valley 68 meters below.

As a rule, the differences at all sites tend to be smallest during the cool months and largest during the warm months. Of the 17 sites examined, only 3 have mean differences greater then ±1mm when outliers are removed. The average standard deviation and RMS differences for all sites with outliers removed are 1.5 and 1.8 mm respectively. Coastal sites at latitudes between the equator and ± 30$^{o}$ climates tend to have the largest scatter (see Pago Pago, AS, Cape Canaveral, FL, and Hilo, HI).

## 3. FACTORS IMPACTING THE RESULTS

Both GPS and radiosonde observation errors impact the results and conclusions of this study. GPS

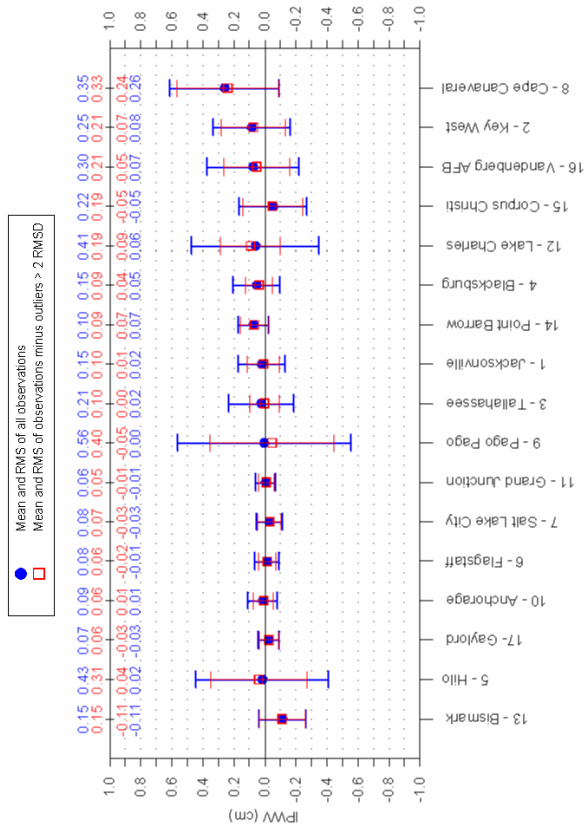


**Figure 6. Data represented in Tables 2 and 3 sorted by mean difference between radiosonde and GPS IPW observations. The raw (unedited) statistics are plotted in blue, while statistics derived by removing outliers (all values > ±2 RMSD) are plotted in red.**

IPW observation errors were discussed in Gutman et al., 2004b. and every effort was made to identify and exclude questionable GPS measurements from this study.

Radiosondes are also subject to systematic and random errors (Zipser and Johnson, 1998, Guichard et al., 1999). In recent years, sources of systematic errors in relative humidity and temperature measurements have been identified and to some extent mitigated with varying degrees of success (Turner et al., 2003). These efforts have resulted in superior sensor performance and data correction techniques that have measurably improved data quality and reliability. However, detection of random errors remains a difficult problem, primarily due to the lack of redundant or independent observations from measurement systems with comparable accuracy.

Another factor is transport of the radiosonde away from the GPS site such that the two systems are not simultaneously sampling the same air mass. This is illustrated in Figure 7 which shows an IPW time series for the Sterling, VA Upper-Air site (IAD) compared to two nearby GPS-Met sites: Leesburg, VA (ZDC1) and the U.S. Naval Observatory (USNO).

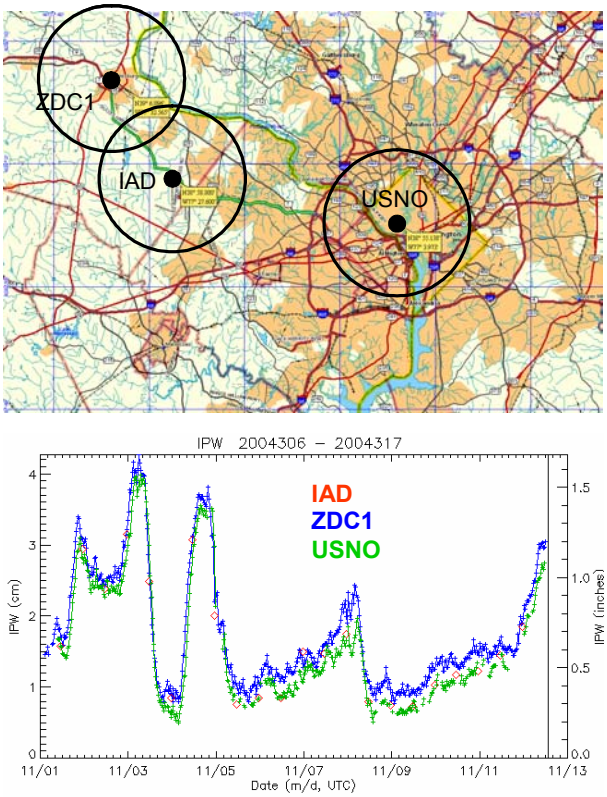


**Fig 7. IPW time series comparing radiosondes launched at Sterling, VA (IAD) with IPW measured at Leesburg, VA (ZDC1) 15.3 km northwest of IAD and the U.S. Naval Observatory in Washington, DC (46.1 km east-southeast). Prevailing winds transport the radiosondes launched at Sterling eastward, resulting in better comparisons with USNO then ZDC1 on occasion. The circles surrounding the sites represents the nominal field of view of the GPS antenna, 11 km.**

Factors including miscalibration, mishandling of sensors, or bad lots of sensors generally fall into the category of random errors. Considering the limited number of moisture soundings, and the growing importance of these observations for weather forecasting, climate monitoring, and satellite calibration and validation, it is important that these errors be found and corrected, or at the least identified, and that this information is available to the user community so that the impact of these events can be minimized and contained.

## 4. USING GPS TO QUALITY CONTROL RADIOSONDE MOISTURE OBSERVATIONS

Even if we cannot anticipate certain radiosonde moisture sounding problems, the availability of an independent observation of comparable accuracy makes it possible to reliably identify and flag questionable observations for the first time. A real-time demonstration of this capability is underway at Sterling, VA (IAD) and Caribou, ME in collaborative effort between the Observing Systems Branch of the NWS Office of Operational Systems, the Science Plans Branch of the NWS Office of Science and Technology, and the GPS-Met Observing Systems Branch of the NOAA Forecast Systems Laboratory.

Preliminary results are encouraging. Continuous comparisons between Sterling and Leesburg, VA have been carried out since February 19, 2004. The IPW comparisons at IAD are made using GPS data from Federal Aviation Administration Wide Area Augmentation System (WAAS) control station at Leesburg, VA (ZDC1), and surface meteorological data from the ASOS at Washington Dulles International Airport (KIAD).

- # synoptic periods = 534
- # soundings = 520
- # comparisons = 446
- % comparisons = 85.8
- % missing comparisons due to no GPS = 35.1
- % missing comparisons due to no ASOS = 64.9

Identical comparisons have been carried out at Caribou, ME since July 22, 2004. The IPW comparisons at CAR are made using GPS data from the NOAA/FSL GPS-Met system at the Upper-Air Site and surface meteorological data from the nearby ASOS (KCAR).

- # synoptic periods = 228
- # soundings = 224
- # comparisons = 208
- % comparisons = 92.9
- % missing comparisons due to no GPS = 18.8
- % missing comparisons due to no ASOS = 100%

Table 3. Probability of detection (POD), false alarm rate (FAR), critical success index (CSI), and bias calculations for Caribou, ME.

| | |
|---|---|
| POD | 0.975369458 |
| FAR | 0.024630542 |
| CSI | 0.951923077 |
| BIAS | 1.0 |

$$POD = \frac{x}{x+y} \quad (4)$$

$$FAR = \frac{z}{x+z} \quad (5)$$

$$CSI = \frac{x}{x+y+z} \quad (6)$$

$$BIAS = \frac{x+z}{x+y} \quad (7)$$

Where:
x = number of good soundings identified as good
y = number of good soundings identified a bad
z = number of bad sondes identified as good

**ACKNOWLEGMENTS**

The idea of using GPS as a way to evaluate the accuracy of radiosonde moisture soundings was originally proposed by Ralph Peterson. We wish to thank Carl Bower of the National Weather Service and Chuck Wade of the National Center for Environmental Prediction for their insight, and stimulating discussions regarding the utility of using GPS for this purpose.

**REFERENCES**

Bevis, M., S. Businger, T. Herring, C. Rocken, R. Anthes, R. Ware, 1992. GPS meteorology: remote sensing of the atmospheric water vapor using the global positioning system. J. Geophys. Res., Vol. 97, No. D14, 75-94.

Bevis, M, S Businger, S Chiswell, T Herring and R Anthes, 1994. GPS meteorology---mapping zenith wet delays onto precipitable water, J Appl Meteorology, 33(3), 379-386.

Duan, J.M., M. Bevis, P. Fang, Y. Bock, S.R. Chiswell, S. Businger, C. Rocken, F. Soldheim, R.H. Ware, T.A. Hering, and R.W. King, 1996. Remote Sensing Atmospheric Water Vapor using the Global Positioning System, J. Appl. Meteor, 35, 830-838.

Eyre, J.R., 1994. Assimilation of radio occultation measurements into a numerical weather prediction system. ECMWF Tech Memo, 199, Reading, UK.

Fitzgibbon, J. and J. Facundo, 2005. Testing Radiosonde Replacement System (RRS) Radiosondes – Part 1, 9th Symposium on Integrated Observing and Assimilation Systems for the Atmosphere, Oceans, and Land Surface, paper 11.5, San Diego, CA Jan 9-13 available in combined reprints on CD-ROM.

Guichard, F., D. B. Parsons, and E. R. Miller, 1999. The radiative impact of a correction for a sonde humidity bias over the Tropical Western Pacific. Ninth ARM Science Team Meeting Proceedings, San Antonio, Texas, March 22-26, 1-7.

Gutman, S.I., S.R. Sahm, S.G. Benjamin, B.E. Schwartz, K.L. Holub, J.Q. Stewart, and T.L. Smith, 2004. Rapid Retrieval and Assimilation of Ground Based GPS Precipitable Water Observations at the NOAA Forecast Systems Laboratory: Impact on Weather Forecasts. Journal of the Meteorological Society of Japan, Vol. 82, No. 1B, 351-360.

Gutman, S.I., S.R. Sahm, S.G. Benjamin, T.L. Smith, 2004b. GPS water vapor observation errors. 8th Eighth Symposium on Integrated Observing and Assimilation Systems for Atmosphere, Oceans, and Land Surface, paper 8.3, Seattle, WA Jan. 11-15 available in combined reprints on CD-ROM.

Kursinski, E.R., G.A. Hajj, and K.R. Hardy, 1993. Temperature or moisture profiles from radio occultation measurements. 8th Symposium on Meteorologigical Observations and Instrumentation, paper JP2.14 Anaheim, CA Jan 17-22, J153-J158.

McMillin, L.M., J. Zhao, R.V.R. Mundakkara Kovilakom, S.I. Gutman, and J.G. Yoe, 2005. AIRS water vapor validation using RAOBs and GPS, 9th Symposium on Integrated Observing and Assimilation Systems for the Atmosphere, Oceans, and Land Surface, paper 1.3, San Diego, CA Jan 9-13 available in combined reprints on CD-ROM.

Saastamoinen, J., 1972. Introduction to practical computation of astronomical refraction, Bull. Geod., 106, 383-397.

Smith, E.K. and S. Weintraub, 1953. The constants in the equation of atmospheric refractive index at radio frequencies. Proceedings of the Institute of Radio Engineers, Vol. 41, No. 8, pp. 1035-1037.

Turner, D.D., B.M. Lesht, S.A. Clough, J.C. Liljegren, H.E. Rivercomb, & D.C. Tobin, 2003: Dry Bias Variability in Vaisala RS80-H radiosondes: The ARM experience, J. Atmos. Oceanic Technol., 20, 117-132.

Wolfe, D.E. and S.I. Gutman, 2000. Development of the NOAA/ERL Ground-Based GPS Water Vapor Demonstration Network: Design and Initial Results, J. Atmos. Ocean. Technol, 17, 426-440.

Yuan, L., R. Anthes, R. Ware, C. Rocken, W. Bonner, M. Bevis, and S. Businger, Sensing climate change using the Global Positioning System, J. Geophys. Res., 98, 14,925-14,937, 1993.

Zipser, E. J., and R. H. Johnson, 1998. Systematic errors in radiosonde humidities a global problem? Preprints, 10th Symp. on Measurements, Observations and Instrumentation, Phoenix, Arizona, Amer. Meteor. Soc., 72-73.